

# Modal Identification in Presence of Noise Using an Optimisation Approach

C. Thonon, J.C. Golinval

LTAS, Vibrations et Identification des Structures, University of Liège, Belgium

e-mail : c.thonon@ulg.ac.be, jc.golinval@ulg.ac.be

## Abstract

This paper deals with the problem of modal parameter identification when the measurements are perturbed by unknown but bounded noise. It is well known that the classical Total Least Square (TLS) solution is the most accurate one, but that it is quite sensitive to data perturbations. This feature is a big drawback since it is desirable that the estimated modal parameters should not vary when perturbations on measurements change.

An optimisation technique suited to so-called second-order cone programs [2] is proposed and tested. This method sets the identification problem in a MIN-MAX formulation [1] and uses an iterative interior-point primal-dual potential reduction algorithm [3, 4]. The residual error is first maximised over the set of possible perturbations leading thus to a worst-case residual error. Then, it is minimised over the set of identification variables. This procedure guarantees the robustness of the solution in the sense that no perturbation of the considered set could make the residual error bigger. This robustness is obtained to the detriment of an absolute accuracy. A good compromise between robustness and accuracy may be found through the prior resolution of the associate TLS problem.

The optimisation program is tested in the case of a clamped-free beam for which closed-form solutions are available. A comparison with the TLS solution is also performed.

## 1. Introduction

Identification of modal parameters using experimental vibration data often leads to the resolution of an overdetermined linear system of equations :

$$\mathbf{A}\mathbf{x} = \mathbf{b} \quad (1)$$

where matrix  $\mathbf{A}_{n \times m}$  and vector  $\mathbf{b}_n$  collect a set of measurement dependent coefficients. Both  $\mathbf{A}$  and  $\mathbf{b}$  are perturbed by what is commonly called "noise". It can be due to the experimental set up itself, to the data acquisition procedure or simply to bad environmental conditions during testing when the measurements are done on industrial sites. That is why equation (1) is rewritten as

$$(\mathbf{A} + \Delta\mathbf{A})\mathbf{x} = \mathbf{b} + \Delta\mathbf{b} \quad (2)$$

in which the implicit dependency in the unknown perturbations  $\Delta\mathbf{A}$  and  $\Delta\mathbf{b}$  appears.

The aim of the research is to develop and test the ability of an optimisation tool to solve (2) iteratively so that unknown but bounded perturbations can be directly taken into account during the modal identification step.

Denoting the extended perturbation matrix  $\Delta = [\Delta\mathbf{A} \ \Delta\mathbf{b}]$ , equation (2) is transformed into a min-max problem such that

$$\min_{\mathbf{x}} \max_{\|\Delta\|_F \leq \rho} \| (\mathbf{A} + \Delta\mathbf{A})\mathbf{x} - (\mathbf{b} + \Delta\mathbf{b}) \| \quad (3)$$

in which subscript  $F$  states for the Frobenius norm and where  $\rho$  is the considered (not necessarily small) range of action of the perturbation which bounds the norm of  $\Delta$  [1].

In this form, the objective function matches the residual error of problem (2) except that it is computed in the worst case inside the sphere of perturbation variation. Consequently, at the end of the optimisation process, the objective function does not tend to zero but to an upper limit value that no perturbation  $\Delta$  in the sphere of radius  $\rho$  could make bigger. In that sense, the method proposed here does not lead to an "accurate" solution like a least squares solution. But, in opposition to least squares approaches, the solution  $\mathbf{x}$  obtained here is less sensitive to noise. This feature shows the robustness of the method and should be very interesting in the field of modal identification.

## 2. Uncertainty model

The radius  $\rho$  of the perturbation sphere cannot be known a priori. If it is over estimated, the solution  $\mathbf{x}$  should be more robust, but also quite less accurate. If it is under estimated, the loss of robustness can lead to instabilities in the identification of the parameters. In particular, when  $\rho \rightarrow 0$ , problem (3) turns out into the associate Total Least Squares (TLS) problem which is known to be very sensitive to data perturbations.

A simple and automatic way to correctly evaluate the radius  $\rho$  in a given application [1] is to compute the TLS solution  $(\mathbf{x}^*, \Delta \mathbf{A}^*, \Delta \mathbf{b}^*)$ . This leads generally to a good compromise between accuracy and robustness. The nominal data, center of the perturbation sphere are then taken as

$$\mathbf{A}^* = \mathbf{A} + \Delta \mathbf{A}^* \quad \text{and} \quad \mathbf{b}^* = \mathbf{b} + \Delta \mathbf{b}^* \quad (4)$$

and the radius  $\rho$  to consider is given by the norm of the TLS correction matrix making the system of equations consistent :

$$\rho = \rho_{TLS} = \| (\Delta \mathbf{A}^*, \Delta \mathbf{b}^*) \|_F \quad (5)$$

But, if the TLS solution was about to be quite wrong, it would be recommended to keep the measured data  $(\mathbf{A}, \mathbf{b})$  as nominal data. Otherwise, the initial problem to solve could be entirely misrepresented.

## 3. Optimisation method [1,2]

In the following, the radius of perturbation  $\rho$  will be taken equal to one. If it is not the case, a preliminary scaling step of the problem is necessary :

$$\min_{\mathbf{x}} \max_{\|\Delta\|_F \leq 1} \| (\mathbf{A}' + \Delta \mathbf{A}') \mathbf{x} - (\mathbf{b}' + \Delta \mathbf{b}') \| \quad (6)$$

$$\text{with } \mathbf{A}' = \frac{\mathbf{A}}{\rho} \quad \text{and} \quad \mathbf{b}' = \frac{\mathbf{b}}{\rho}$$

### 3.1 Worst-case residual error

Applying the triangular inequality principle, the worst-case residue becomes (for  $\rho = 1$ ):

$$\begin{aligned} & \varepsilon_{max}(\mathbf{A}, \mathbf{b}, \mathbf{x}) \\ = & \max_{\|\Delta\|_F \leq 1} \| (\mathbf{A}' + \Delta \mathbf{A}') \mathbf{x} - (\mathbf{b}' + \Delta \mathbf{b}') \| \\ = & \| \mathbf{A}' \mathbf{x} - \mathbf{b}' \| + \sqrt{\mathbf{x}^T \mathbf{x} + 1} \end{aligned} \quad (7)$$

This function has now to be minimized over the set of parameters  $\mathbf{x}$  to be identified.

### 3.2 Primal optimisation problem

Using two additional variables  $\lambda$  and  $\tau$ , the primal optimisation problem transforms into [1]

$$\begin{aligned} & \min_{\mathbf{x}, \lambda, \tau} \quad \lambda \\ & \text{with} \quad \| \mathbf{A} \mathbf{x} - \mathbf{b} \| \leq \lambda - \tau \\ & \text{and} \quad \| (\mathbf{x}^T, 1) \| \leq \tau \end{aligned} \quad (8)$$

Written in this form, the objective function is linear and the constraints are conic. It is part of the class of Second Order Cone Programs (SOCP) [2]. Nesterov and Nemirovsky [4] showed that such problems can be efficiently solved using an iterative interior point algorithm which minimises a potential function combining both primal and dual spaces.

Such a method is used in the field of control and should be well adapted to identification for the following reasons :

- the analytical and differential features of the problem can be exploited and reduce the iteration cost;
- the number of iterations is independent of the size  $n$  of the system;
- the convergence is monotonic, assuring a stable and feasible solution ; this is due to the progression by interior points;
- the problem takes a nearly convex form guaranteeing a global minimum.

If one collects the primal variables in vector  $\mathbf{y}^T = (\mathbf{x}^T, \lambda, \tau)$ , the problem is rewritten in the standard SOCP form [2]:

$$\begin{aligned} & \min_{\mathbf{y}} \mathbf{f}^T \mathbf{y} \\ & \text{with} \quad \| \mathbf{A}_1 \mathbf{y} - \mathbf{b}_1 \| \leq \mathbf{c}_1^T \mathbf{y} \\ & \text{and} \quad \| \mathbf{A}_2 \mathbf{y} - \mathbf{b}_2 \| \leq \mathbf{c}_2^T \mathbf{y} \end{aligned} \quad (9)$$

where  $\mathbf{A}_1 \in \mathcal{R}^{n \times m+2}$ ,  $\mathbf{A}_2 \in \mathcal{R}^{m+1 \times m+2}$ ,  $\mathbf{b}_1 \in \mathcal{R}^n$ ,  $\mathbf{b}_2 \in \mathcal{R}^{m+2}$ ,  $\mathbf{c}_1 \in \mathcal{R}^{m+2}$ ,  $\mathbf{c}_2 \in \mathcal{R}^{m+2}$  et  $\mathbf{f} \in \mathcal{R}^{m+2}$ .

### 3.3 Associate dual formulation

The dual formulation of problem (9) is [2]

$$\begin{aligned} & \max_{\mathbf{z}} -(\mathbf{b}_1^T \mathbf{z}_1 + \mathbf{b}_2^T \mathbf{z}_2) \\ & \text{with} \mathbf{A}_1^T \mathbf{z}_1 + w_1 \mathbf{c}_1 + \mathbf{A}_2^T \mathbf{z}_2 + w_2 \mathbf{c}_2 = \mathbf{f} \\ & \quad \| \mathbf{z}_1 \| \leq w_1, \\ & \quad \text{and} \quad \| \mathbf{z}_2 \| \leq w_2 \end{aligned} \quad (10)$$

The dual variables are collected in vector  $\mathbf{Z}^T = (\mathbf{z}_1^T, w_1, \mathbf{z}_2^T, w_2)$ .

### 3.4 Duality gap

The difference between the primal objective and the dual one is called the duality gap [3, 4]. For each admissible pair  $(\mathbf{y}, \mathbf{Z})$  (i.e. a pair verifying the primal and the dual constraints of the optimisation problem), the duality gap value is given by

$$\eta(\mathbf{y}, \mathbf{Z}) = \mathbf{f}^T \mathbf{y} + (\mathbf{b}_1^T \mathbf{z}_1 + \mathbf{b}_2^T \mathbf{z}_2) \quad (11)$$

This function is always positive and tends to zero when the solution goes to the optimal point.

### 3.5 Barrier functions

The interior point feature of the method is obtained through the moving of all inequality constraints into the objective function under the form of barrier functions [4]. Logarithmic barriers are built for each conic constraint in such a way :

$$B(\mathbf{u}, t) = \begin{cases} -\log(t^2 - \mathbf{u}^T \mathbf{u}) & \forall \|\mathbf{u}\| < t \\ \infty & , \text{otherwise} \end{cases} \quad (12)$$

Barriers act thus as penalty terms preventing from moving outside the feasible space. Their Jacobian, Hessian and inverse Hessian may be easily computed in the following analytical form :

$$\nabla B(\mathbf{u}, t) = \frac{2}{t^2 - \mathbf{u}^T \mathbf{u}} \begin{bmatrix} \mathbf{u} \\ -t \end{bmatrix} \quad (13)$$

$$\nabla^2 B(\mathbf{u}, t) = \frac{2}{(t^2 - \mathbf{u}^T \mathbf{u})^2} \begin{bmatrix} (t^2 - \mathbf{u}^T \mathbf{u})\mathbf{I} & -2t\mathbf{u} \\ -2t\mathbf{u}^T & t^2 + \mathbf{u}^T \mathbf{u} \end{bmatrix} \quad (14)$$

$$\nabla^2 B(\mathbf{u}, t)^{-1} = \frac{1}{2} \begin{bmatrix} (t^2 - \mathbf{u}^T \mathbf{u})\mathbf{I} + 2\mathbf{u}\mathbf{u}^T & 2t\mathbf{u} \\ 2t\mathbf{u}^T & t^2 + \mathbf{u}^T \mathbf{u} \end{bmatrix} \quad (15)$$

### 3.6 Primal-dual algorithm

Primal and dual optimisation problems take quite the same form. It is thus easy to handle them in the same time through the use of a potential function combining the duality gap which is to be minimised and the barrier functions. The potential function prescribed by Nesterov and Nemirovsky [4] is defined as

$$\phi(\mathbf{y}, \mathbf{Z}) = (4+2\nu) \log \eta + B_{1,P} + B_{2,P} + B_{1,D} + B_{2,D} \quad (16)$$

where  $B_{1,P}$ ,  $B_{2,P}$ ,  $B_{1,D}$ ,  $B_{2,D}$  denote the barrier functions associated to the four primal and dual conic constraints ;  $\nu$  is a numerical parameter allowing to tune the relative weight of the  $\eta$  term and of the penalty terms.

The final form of the optimisation problem results in an unconstrained minimisation problem :

$$\min_{\mathbf{y}, \mathbf{Z}} \phi(\mathbf{y}, \mathbf{Z}) \quad (17)$$

All constraints are included in the objective function except for the equality constraint of the dual problem. This last constraint will have to be imposed at each iteration during the search direction computation step.

#### 3.6.1 Search direction

Starting from a strictly admissible pair  $(\mathbf{y}, \mathbf{Z})$  and at each iteration, the primal and dual search directions  $\delta\mathbf{y}$  and  $\delta\mathbf{Z}$  must stay correctly paired. This can be achieved if the equality constraint of dual problem (10) is verified.

Thus the search direction step combines two matrix equations [2, 4] :

$$\begin{bmatrix} \mathbf{H}^{-1} & \overline{\mathbf{A}} \\ \overline{\mathbf{A}}^T & \mathbf{0} \end{bmatrix} \begin{bmatrix} \delta\mathbf{Z} \\ \delta\mathbf{y} \end{bmatrix} = \begin{bmatrix} -\mathbf{H}^{-1}(\theta\mathbf{Z} + \mathbf{g}) \\ \mathbf{0} \end{bmatrix} \quad (18)$$

with

$$\mathbf{H} = \begin{bmatrix} \nabla^2 B_{1,D} & \mathbf{0} \\ \mathbf{0} & \nabla^2 B_{2,D} \end{bmatrix} \quad (19)$$

$$\mathbf{g} = \begin{bmatrix} \nabla B_{1,D} \\ \nabla B_{2,D} \end{bmatrix} \quad (20)$$

and  $\theta = (4 + 2\nu)/\eta$ .

The first equation corresponds to a quasi-Newton type direction for problem (17) : the term  $(4 + 2\nu) \log \eta$  is concave and its negative contribution to the hessian is thus neglected. The second equation results from the differentiation of the equality constraint.

#### 3.6.2 Plane search

The current point is updated by minimizing the potential function  $\phi$  in the plane defined by the paired search directions  $(\delta\mathbf{Z}^T, \delta\mathbf{y}^T)$ :

$$\min_{p,q} \phi(\mathbf{y} + p\delta\mathbf{y}, \mathbf{Z} + q\delta\mathbf{Z}) = 0 \quad (21)$$

The primal and dual step lengths  $p$  and  $q$  vary between 0 and an upper limit corresponding to the barrier crossings.

## 4. Application example

The method was tested on simulated measurements of a clamped-free bending beam. The frequency response function (FRF) at the free end of the beam was generated by modal superposition. Modal damping ratios were set to 2%. The first 3 exact eigenfrequencies are 8.36 Hz, 52.35 Hz and 146.58 Hz. For instance, the impulse response function (IRF) at the end of the beam ( $h_{1,1}$ ) is shown at figure 1.

The modal identification was made using the Least Squares Complex Exponential method (LSCE)[5, 6]. LSCE leads to the resolution of a system like (1) where matrix  $A$  and vector  $b$  are made of digitalised impulse response functions. The identification of the first 3 eigenfrequencies was performed using

1. the optimisation method (OPTI),
2. the TLS method.

### 4.1 Robustness and accuracy

In order to compare both methods, several tests were realized. At each time, the signal was perturbed by white noise with a signal to noise ratio (SNR) of

$$SNR = 10 \log \frac{\sigma_{h_{1,1}}^2}{\sigma_{noise}^2} = 14 \text{ dB} \quad (22)$$

This random perturbation always led to a rather small TLS correction :  $\rho_{TLS} \simeq 4.2 \cdot 10^{-4}$ . Figure 1 displays the exact signal along with the added perturbation. Table 1 gives the results of 3 tests. Regarding to the

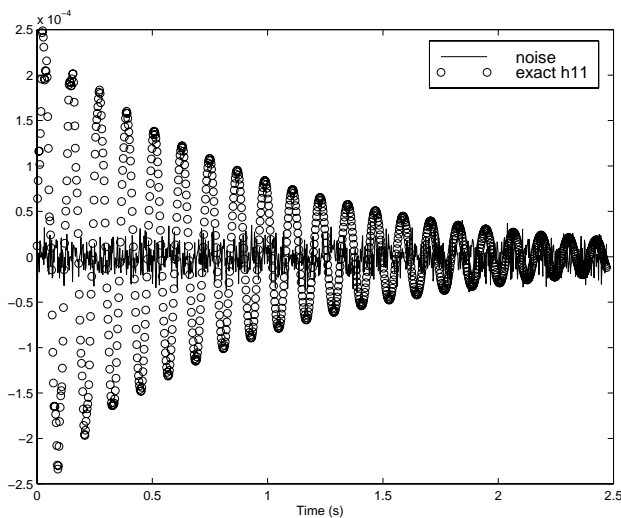


Figure 1: Exact signal and added white noise

TLS method, it is observed that the results are more

No	OPTI		TLS	
	freq. (Hz)	$\epsilon$ (%)	freq. (Hz)	$\epsilon$ (%)
1	8.62	2.46	8.33	-3.26
	54.05	8.35	52.69	2.99
	131.83	2.47	131.89	-0.4
2	8.42	7.34	8.74	1.39
	53.03	10.96	50.70	-6.02
	152.04	4.67	142.70	-1.06
3	7.98	13.99	11.36	34.35
	53.13	1.6	47.04	-2.15
	164.31	3.08	164.26	0.07

Table 1: OPTI / TLS comparison

dispersed. The method leads to an accurate solution in the sense that the residue of the system of equations is zero, but the final solution strongly depends on the chosen recorded sample used for the identification. The TLS method sometimes leads to negative values for the modal damping coefficients. The corresponding poles would normally be considered in practice as numerical poles and would be rejected.

At the opposite, the OPTI solution is characterized by a smaller standard deviation and always gives positive damping ratios. However, the latter may sometimes be poorly estimated. In this particular example, it can be explained by

- the relatively high noise level,
- a too small frequency resolution for the first peak,...

For each test, the optimisation method always converges in 7 or 8 iterations. Figure 2 displays an example of typical convergence curves for the objective and the potential functions. It also illustrates the convergence of the duality gap.

### 4.2 Perturbation radius influence

Starting from exact noise free measurements, the perturbation radius  $\rho$  of the OPTI method is progressively increased. Doing this, a larger perturbation around the data is taken into account and the accuracy of the solution decreases. As an example, the evolution of an identified parameter when  $\rho$  grows is displayed in figure 3. Again, the robustness of the method appears.

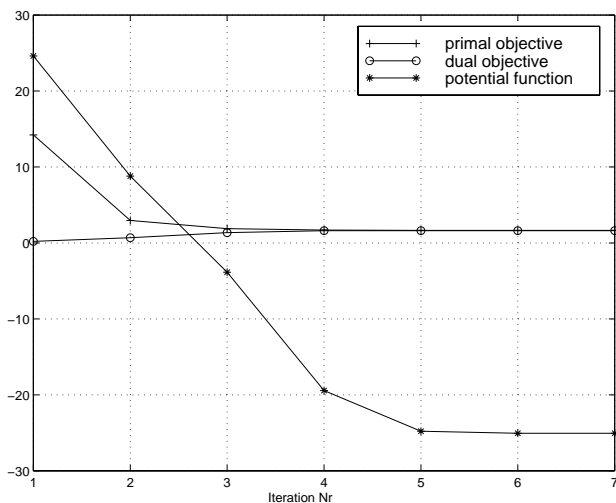


Figure 2: Convergence curves

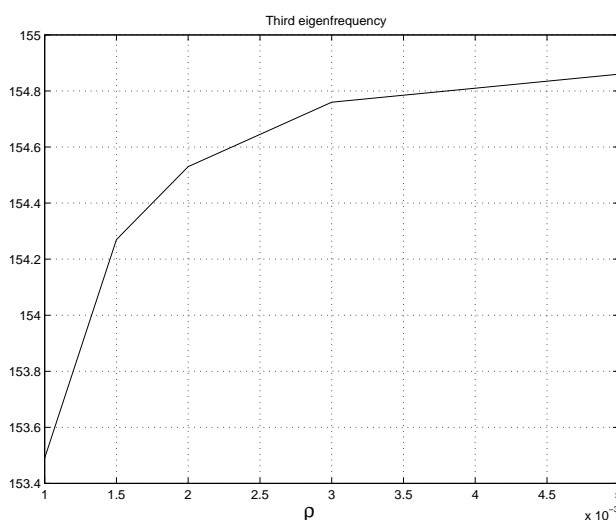


Figure 3: Radius  $\rho$  influence on third frequency

## 5. Conclusion and perspectives

An optimisation toll for the identification of modal parameters was tested on the basis of an analytical test case.

An improvement of the algorithm has still to be done for the computation of the step lengths during the plane search. At present, the plane search computation cost is prohibitive because it is done by a dichotomy procedure. The analytical feature of the problem should better be exploited to obtain approximate step lengths.

In the future, other identification techniques will be tested in concordance with this optimisation solver. This tool will also be tested for structural model updating since it leads to solutions much more insensitive to noise.

## References

1. L. El Ghaoui, H. Le Bret, *Robust Solutions to Least-Squares Problems with Uncertain Data*, SIAM J. on Matrix Analysis and Applications, (October, 1997).
2. M.S. Lobo, L. Vandenberghe, S. Boyd, H. Le Bret, *Applications of Second-order Cone Programming*, Linear Algebra and Applications, (1998).
3. L. Vandenberghe, S. Boyd, *Semidefinite Programming*, SIAM Review, (March, 1996).
4. Y. Nesterov, A. Nemirovsky, *Interior point polynomial methods in convex programming : Theory and applications*, SIAM, Philadelphia, PA, (1994).
5. W. Heylen, S. Lammens, P. Sas, *Modal Analysis Theory and Testing*, ISMA24 course, (September, 1999).
6. Maia, Silva, He, Lieven, Lin, Skingle, To, Urgueira, *Theoretical and Experimental Modal Analysis*, (1997).